Analysis of wheel-rail contact stresses

Mohamed Hafez Fahmy Aly
Transportation Department, Faculty of Eng. Alexandria University, Alexandria, Egypt

Variation of the wheel-rail contact areas and contact stresses in a railway system, due to dynamic behavior of the rail vehicles, affect the rail wear and consequently the rail fatigues life. The rolling contact fatigue damage is produced on the rail-running surface by the dynamic behavior of the wheel-set rolling on the rail. Rail damage is a significant cause of rail replacement. The purposes of this paper are to analyze the wheel-rail contact stresses and investigate the effects of these stresses on the rail life. The dynamic behavior of the rail vehicle was analyzed. Factors affecting wheel-rail contact areas have been investigated. The wheel-rail contact areas for different wheel contact positions were estimated. Factors affecting the wheel-rail contact stresses have been analyzed. The contact stresses for different wheel positions were also determined. Finally, relationships between the contact stresses and the rail life have been investigated.

تعتبر التغييرات في مساحات التلامس بين عجلات القطارات والقضبان في أنظمة السكك الحديدية ، وكذلك الاجهادات التلامسية والناتجة عن الحركة الديناميكية للعربات، من العوامل الرئيسية في التأثير على عمر قضبان السكك الحديدية وتآكلها. فمن الأسباب الرئيسية لتجديدات القضبان بالسكك الحديدية هو تلف وكسور وتآكل السطوح العلوية للقضبان والذي قد ينتج عن الحركة الديناميكية لعجلات عربات السكك الحديدية. ولذلك فإن هذا البحث يهدف بصورة رئيسية إلي دراسة وتحليل الاجهادات التلامسية بين عجلات قطارات السكك الحديدية والقضبان، وكذلك دراسة تأثير هذه الاجهادات على عمر قضبان السكك الحديدية .وللوصول إلى هذا الهدف تم تحليل الحركة الديناميكية لعربات السكك الحديدية ،ودراسة العوامل المؤثرة في مساحات التلامس بين العجلة والقضبان .وتم أيضا تحديد مساحات التلامس لأوضاع مختلفة لعجلات عربات السكك الحديدية، وتقييم الاجهادات الناتجة عن هذه المساحات .ولقد تم أيضا دراسة وتحليل العوامل المؤثرة في هذه الاجهادات .وأخيرا تم دراسة وتحليل العلاقة بين الاجهادات التلامسية بين عجلات قطارات السكك الحديدية والقضبان وعمر القضبان نفسها .

Keywords: Railway, Dynamic behavior, Contact area, Contact stresses

1. Introduction

Modern railway development has brought improvements in the design of track, bogies and wheels and also in the maintenance of track and rolling stock. This has resulted in a decrease in wear of rails and increasing of their operational lives. At the same time, economical and logistical demands have introduced increases in train speeds and axle loads leading to increase of contact stresses, and decrease of rail lives.

Wheel-rail contact stresses depend not only on the relative position of the wheel and rail, but also on the axle loads, wheel-rail contact geometry and track curvature and design.

The purposes of this paper are to analyze the wheel-rail contact stresses and estimate their effects on the rail-life.

This paper is divided into five major sections. In the first section analysis of the dynamic behavior of the rail vehicle has been performed. In the second section factors affecting the sinusoidal lateral motion of the wheel-set have been examined. In the third section, factors affecting wheel-rail contact areas have been investigated. The wheel-rail contact areas for different wheel contact positions were also estimated. The fourth section analyzes the wheel-rail contact stresses. The contact stresses for different wheel positions were also determined. In the last section, relationships between the contact stresses and the rail life have been investigated.

© Faculty of Engineering Alexandria University, Egypt.

2. Analysis of the dynamic behavior of rail vehicles

Rail vehicles belong to a class of vehicles, which are supported as well as guided by rail. The profiles of wheel and rail should be designed not only to support the weight of vehicle, but also to perform the guiding function.

Wheel-set flange clearance, typically 5-20 mm to each side, allows the wheel-set to follow a snacking path, sinusoidal path, a path deviating from the centerline of the track by the same amounts. These motions can have significant effects on the dynamic behavior of a vehicle.

The dynamic behavior of rail vehicles is dominated by vibration modes containing motions in lateral direction. The ability of a wheel-set to perform lateral oscillations when rolling along the track is based on the fact that the wheel treads are profiled. Apart from these geometric aspects, the nature of the oscillations is determined by inertia effects, the elastic properties of the suspension and by creep forces in the contact between wheel and rail.

The dynamic behavior of railway vehicles is dependent upon the self centering effect of the wheel-set, which consists of two coned wheels rigidly fixed to an axle, running on parallel rails. This forms a feedback system and it is therefore possible for the wheel-set to become unstable.

The dynamic behavior of railway vehicles in motion can be analyzed in two-direction, vertical and lateral direction. The modes of vertical vibration of the rail vehicle are vertical translation and rotation about the transverse axis or pitch. Fig. 1 illustrates these modes of vertical vibration. Factors affecting the vertical vibration are the vertical alignment of the track, track characteristics, and track stiffness.

The lateral modes of vibration of a railway vehicle can be described as transverse translations and rotation about the vertical axis and rotation about the longitudinal axis. They are called sway, yaw, and roll respectively. Fig. 2 shows these modes of lateral vibrations. Factors affecting the lateral modes of vibrations are the lateral geometric characteristics of track, cross-sectional level, and the deviation of the track gauge.

The three lateral vibrations modes together with the two vertical modes described above can be used to completely describe the dynamic behavior of rail vehicle.

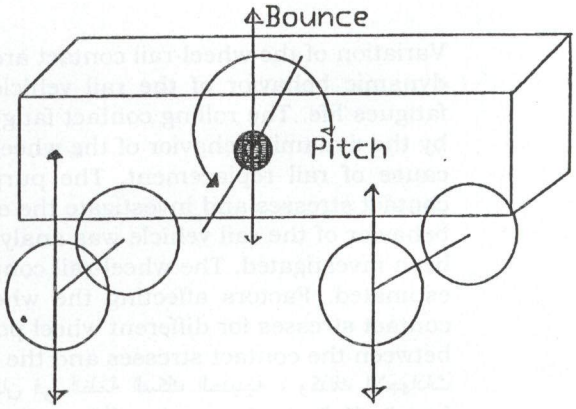

Fig. 1. Modes of vertical vibration of a railway vehicle.

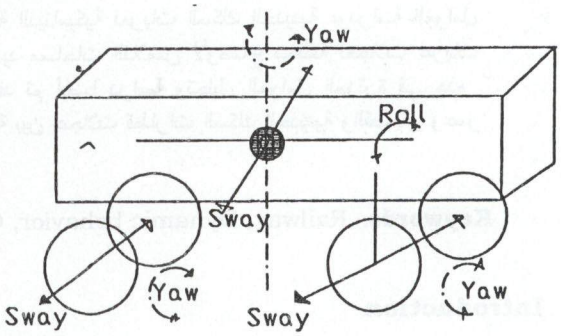

Fig. 2. Modes of lateral vibration of a raillway vehicle.

3. Sinusoidal path of rail vehicles

The understanding of the guidance obtained from the coning of the wheel treads of a railway vehicle goes back to George Stephenson in 1821, and was studied analytically by Klingel in 1883 [1]. Over the years, a further understanding of the way in which detailed changes to the shape of the wheel rim affects the guidance has developed. This has led to the design of a variety of different wheel profiles.

Tread guidance happens when the two conical wheels on a common axle attempt to roll on different rolling radii. When the wheel-

set is rolling centrally within the flange-way clearance, the rolling radii on the two wheels are the same. As the wheel-set deviates to one side of this central position, the wheel approaching flange contact rolls on an increasing radius, whereas the wheel moving away from the flange contact rolls in decreasing radius. Geometrically, one wheel moves forward a greater distance than the other does for each revolution of the axle. This has the effect of causing the axle to rotate about its vertical axis (yaw) and this steers the axle back towards the equal radii position. Unfortunately, the wheel-set overshoots this position, and a sinusoidal lateral motion (snacking path) develops as the wheel-set rolls along the track. This sinusoidal path of the rail wheel-set can be described from the following model [2]:

$$L = 2\,\Pi\,(L_0\, r_1 / \propto)^{0.5}\,. \qquad (1)$$

Where:

- L is the wavelength of the snacking path of the rail vehicle (m),
- L_0 is the track semi-gauge (m),
- r_1 is the rolling radius of wheel, or the adius when both wheels are rolling in equal radii (m),
- $\propto$ is the Tread slope of coned wheel, semi-cone angle.

In order to analyze the effects of angle $\propto$ on the sine-wave length of the rail vehicle path, the models in eq. (1) has been drawn in fig. 3, for r_1 = 50 cm, and L_0= 0.717.5 m (standard gauge). This figure shows that decreasing of semi-cone angle increases of sinusoidal wavelength. The effects of wheel radius, and rail gauge on the wavelength have been investigated in fig. 4 and fig. 5 (for tan $\propto$=1/20, and r_1=50 cm) respectively. These Figures indicate that increasing of wheel radius as well as rail gauges cause increasing in the sinusoidal wavelength. The metric rail gauge (1.067 m) has the minimal wavelength (14.5 m for $\propto$ = 1/20).

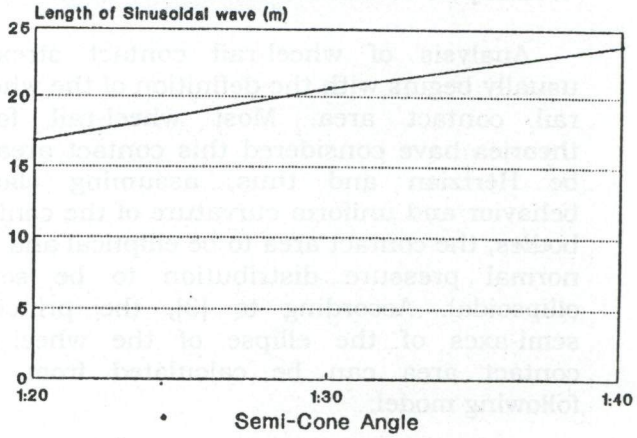

Fig. 3. Effect of semi-cone angle on the sinusoidal wavelength.

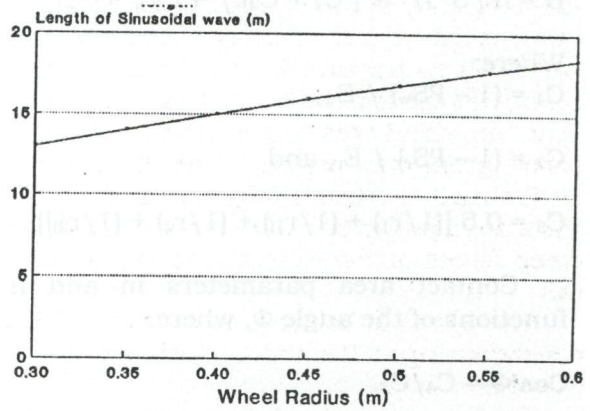

Fig. 4. Effect of wheel radius on the sinusoidal wavelength.

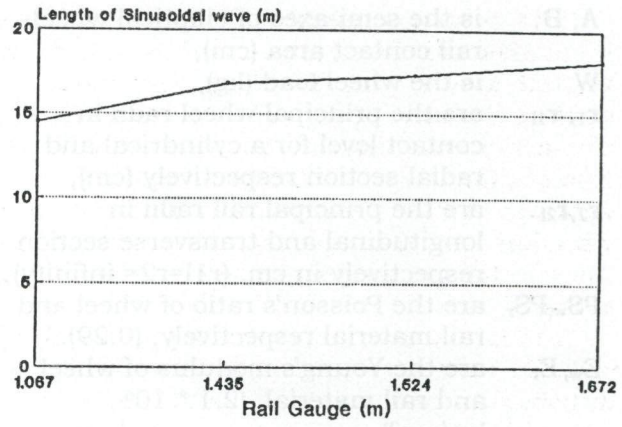

Fig. 5. Effect of rail gauge on the sinusoidal wavelength.

4. Analysis of wheel-rail contact area

Analysis of wheel-rail contact stresses usually begins with the definition of the wheel-rail contact area. Most wheel-rail force theories have considered this contact area to be Hertzian and thus, assuming elastic behavior and uniform curvature of the contact bodies, the contact area to be elliptical and the normal pressure distribution to be semi-ellipsoidal. According to [3], the principal semi-axes of the ellipse of the wheel-rail contact area can be calculated from the following model:

$$A = m [3 \Pi W (C_1 + C_2) / 4 C_3]^{1/3} , \quad (2)$$

$$B = n [3 \Pi W (C_1 + C_2) / 4 C_3]^{1/3} . \quad (3)$$

Where:

$C_1 = (1 - PS_w) / E_w$,

$C_2 = (1 - PS_r) / E_r$, and

$C_3 = 0.5 [(1/r_1) + (1/r_{11}) + (1/r_2) + (1/r_{21})]$

Contact area parameters m and n are functions of the angle Φ, where:

$\text{Cos } \Phi = C_4/C_3$

$C_4 = 0.5 [(1/r_1 - 1/r_{11})^2 + (1/r_2 - 1/r_{21})^2 + 2(1/r_1 - 1/r_{11})(1/r_2 - 1/r_{21}) \text{ Cos } 2\psi]^{1/2}$

A, B is the semi-axes of elliptical wheel-rail contact area (cm),
W is the wheel load (kg),
r_1, r_{11} are the principal wheel radii in contact level for a cylindrical and radial section respectively (cm),
r_2,r_{21} are the principal rail radii in longitudinal and transverse section respectively in cm, (r11=r2= infinity),
PS_w,PS_r are the Poisson's ratio of wheel and rail material respectively, (0.29).
E_w, E_r are the Young's modulus of wheel and rail material, ($2.1 * 10^6$ kg/cm^2),
ψ are the Angle between a plane normal to the wheel axis and rail centerline, (small angle, $\cos 2\psi = 1$).

Table 1 shows the elliptical contact parameters m and n as functions of the angle Φ.

Table 1
Elliptical contact parameters [4]

Φ	M	N
00.5	61.40	0.1018
1.00	36.89	0.1314
1.50	27.48	0.1522
2.00	22.26	0.1691
3.00	16.50	0.1964
4.00	13.31	0.2188
6.00	9.790	0.2552
8.00	7.860	0.2850
10.0	6.604	0.3112
20.0	3.813	0.4123
30.0	2.731	0.4930
40.0	2.136	0.5670
45.0	1.926	0.6040
50.0	1.754	0.6410
55.0	1.611	0.6780
60.0	1.486	0.7170
65.0	1.378	0.7590
70.0	1.284	0.8020
75.0	1.202	0.8460
80.0	1.128	0.8930
85.0	1.061	0.9440
90.0	1.000	1.0000

In order to study the effects of wheel radius on the elliptical wheel-rail contact area, the models in eqs. (2,3) have been drawn in fig. 6. The variation of wheel radius has been defined to range from 45 to 70 cm, and the wheel load (10 tone), and radius of curvature of rail (r_{21} = 30cm) are assumed to be constant. This figure shows that increasing of wheel radius increases the longitudinal semi-axis (A) and decreases the transverse semi-axis (B), and results in increasing the total contact area.

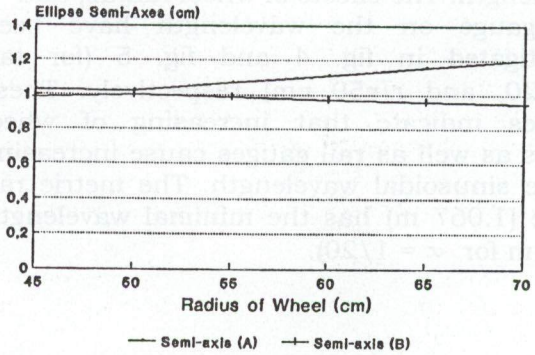

Fig. 6. Effect of wheel radius on wheel-rail contact area.

In order to analyze the effects of radius of curvature of rail on the wheel-rail contact area, the models in eqs. (2, 3) have been drawn in fig. 7 (for W = 10 tone, r_1=50 cm, and r_{2l} varies from 30 to 60 cm). Fig. 7 illustrates that increasing of radius of curvature of rail reduces the longitudinal semi-axis (A), and increases the transverse semi-axis (B). When the radius of curvature of the rail is equal to the wheel radius, (A) is equal to (B) and the contact area will be a circle not an ellipse.

The effects of the wheel load on the wheel-rail contact area have been investigated in fig. 8. This figure indicates that increasing of wheel load results increasing of the semi-axes (A) and (B), and consequently of the wheel-rail contact area.

The effects of wheel and rail material on the contact area have been investigated through the variation of Poisson's ratio of wheel and rail material. As shown in fig. 9, the effect of variation of Poisson's ratio on the wheel-rail contact area is very small.

Finally, It is very important to investigate the effects of the position of wheel-set, lateral shift of wheel-set from the central position within the flange-way clearance, on the wheel-rail contact area. According to the typical cross section configuration of the worn wheel and UIC 50 rail shown in fig. 10, three wheel positions have been assumed, namely, flange contact position, maximum wheel-set shift, and moderate wheel-set shift positions. Flange contact position (case 1) usually occurs in curved track by the outer rail. The maximum wheel shift (case 2) or the moderate shift (case 3) occurs in case of straight track. According to fig. 10, the value of r_1 is assumed to be 1.4 cm, and r_{2l} to be 1.3 cm for case 1, for case 2 r_1 to be 35 cm, and r_{2l} to be 30 cm, and for case 3 r_1 to be 80 cm, and r_{2l} to be 30. The results of the investigation are shown in fig. 11. The minimum contact area occurs in case of flange contact, moderate wheel-set shift requires the maximum wheel-rail contact area.

5. Analysis of wheel-rail contact stresses

The following model, given by Timoshenko and Goodier [6], can be used to determine the wheel-rail contact stresses:

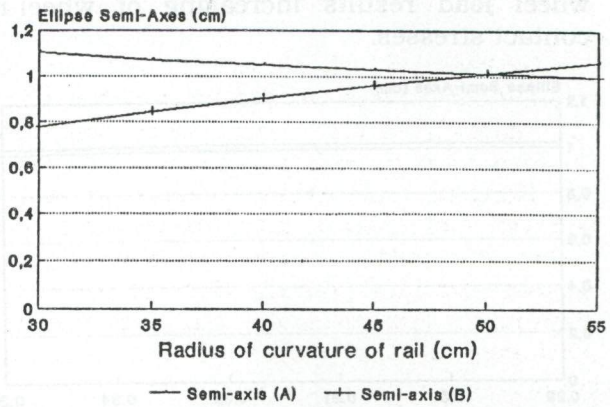

Fig. 7. Effect of radius of curvature of rail on wheel-rail contact area.

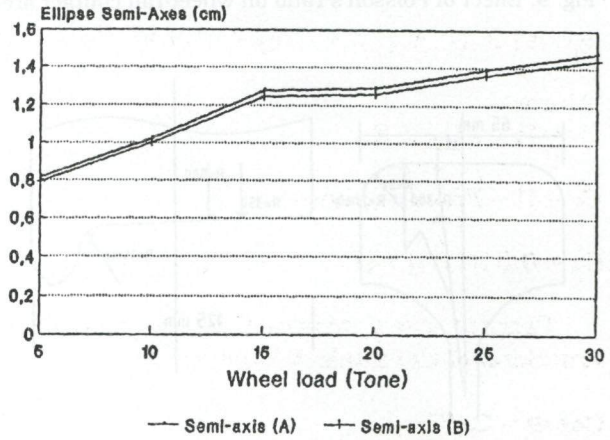

Fig. 8. Effect of radius of curvature of rail on wheel-rail contact area.

$$P_o = 0.418 \left[(W * E) / (2B * r) \right]^{0.5}. \quad (4)$$

Where:

P_o is the Maximum wheel-rail contact stresses in t/m^2,
W is the wheel load in gm,
E is the modulus of elasticity of steel in t/m^2,
B is the semi-transverse contact width of the Hertzian ellipse in mm,
R is given by the following formula:
$1/r = (1/r_1) + (1/r_{2l})$, r_1, and r_{2l} in mm.

In order to study the effects of the wheel load on wheel-rail contact stresses, the models in eqs. (3, 4) have been drawn in fig. 12. The variations of wheel load has been defined to range from 10 to 25 tones, r_1 and r_{2l} are assumed to be constant (r_1 = 80 cm, and r_{2l}=30cm). Fig. 12 indicates that increasing of

wheel load results increasing of wheel-rail contact stresses.

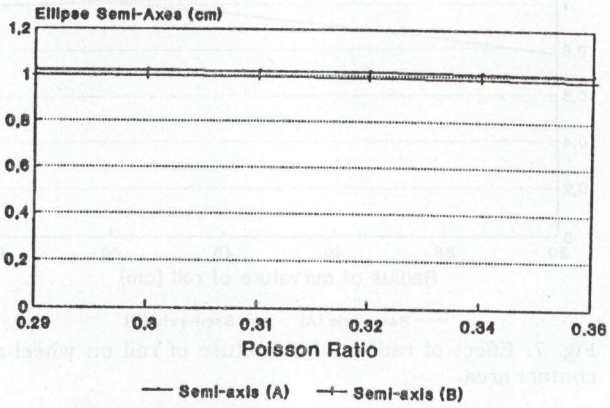

Fig. 9. Effect of Poisson's ratio on wheel-rail contact area.

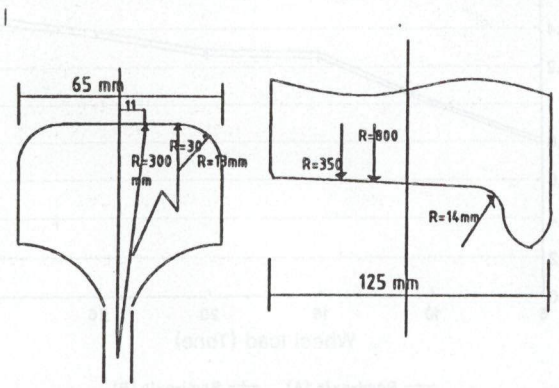

Fig. 10. Typical cross section configuration of UIC 50 rail and worn wheel [5].

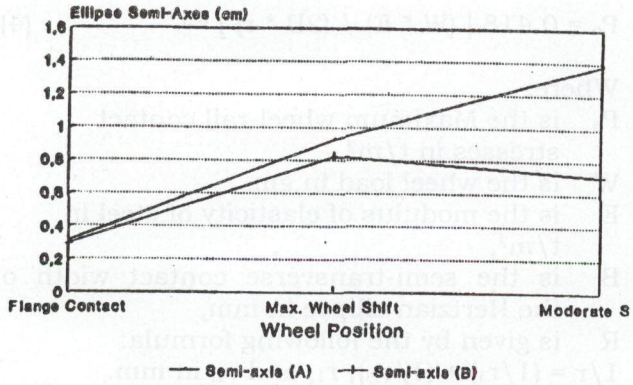

Fig. 11. Effect of radius of wheel position on wheel-rail contact area.

The effects of the position of the wheel-set in the wheel-rail contact stresses have been investigated in fig. 13. This figure shows that the maximum contact stresses occur in flange contact (case 1), while moderate wheel-set shift (case 3) results the minimum wheel-rail contact stresses.

The effects of wheel-rail contact area on the contact stresses, represented in semi-elliptical axes (A) and (B), have been examined in fig. 14. This figure indicates that the contact stresses proportional adversely with the elliptical wheel-rail contact area.

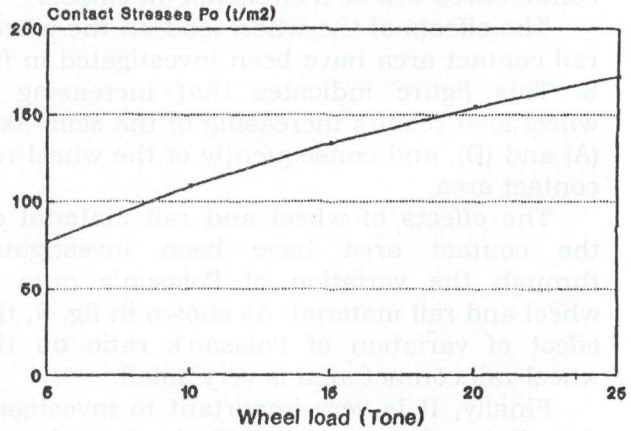

Fig. 12. Effect of wheel load on contact stresses.

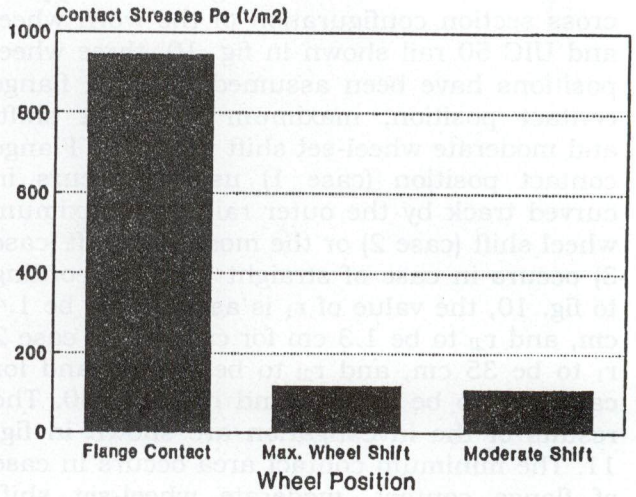

Fig. 13. Effect of wheel position on wheel-rail contact stresses.

Finally, the effects of wheel radius on wheel-rail contact stresses have been investigated in fig. 15. This figure illustrates that reducing of wheel radius results increasing of wheel-rail contact stresses.

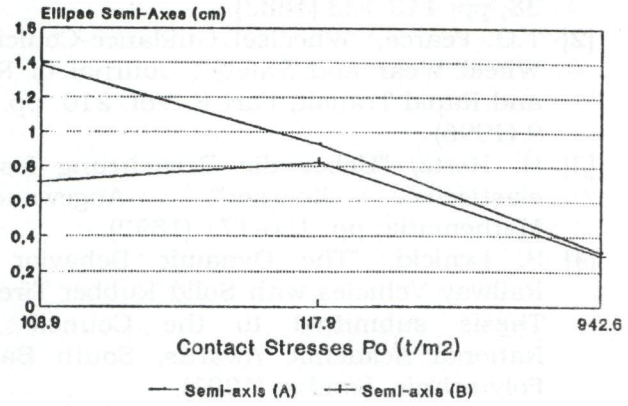

Fig. 14. Effect of wheel-rail contact area on contact stresses.

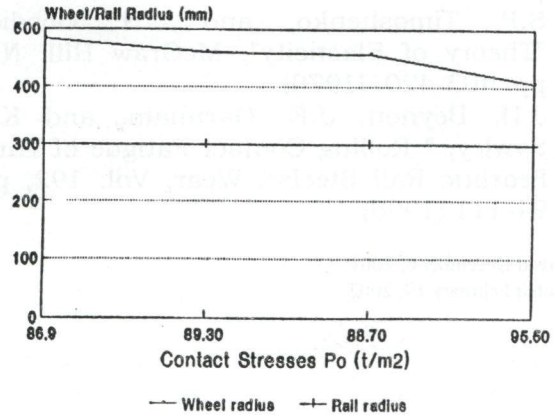

Fig. 15. Effect of wheel radius on wheel-rail contact stresses.

6. Relationship between contact stresses and rail-life

The relationships between contact stresses and rail life have been experimentally investigated in different researches. The following model, given by Beynon and others [7], can be used for investigation purposes:

$$RL_{index} = 127000 - 50\ P_o. \qquad (5)$$

Where:
RL_{index} is the rail life index,
P_o is the contact stresses (t/m^2).

In order to investigate the effects of wheel position on rail life, the models in eqs. (4, 5) have been drawn in fig. 16 (for flange contact, maximum wheel shift, and moderate wheel-shift positions). This figure indicates that outer rails used in curves, which usually have flange contacts, have minimal life than rails used in straight track, which usually have moderates wheel shifts. This shows the importance of using hard steel grade and lubrications of the rails in the curved track. The rails in straight track may have more than 1.5 fold of the lifetime than the rail in curved track.

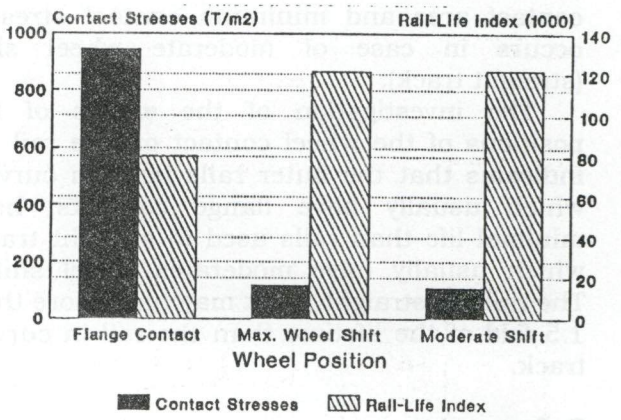

Fig. 16. Effect of wheel position on wheel-rail contact stresses and rail-life.

7. Conclusions

This paper has focussed on the relationships between the dynamic behavior of rail vehicles, the wheel-rail contact areas, the contact stresses, and the rail-life. These elements are interrelated sectors. Reduction in contact areas leads to increasing in contact stresses and decreasing in rail-life. Factors such as wheel-semi-cone angle, wheel radius, rail gauge, radius of curvature of rail, wheel load, wheel and rail materials, and wheel contact positions, affect not only the sinusoidal wheel-set path, but also the wheel-rail contact areas, the wheel-rail contact stresses and consequently the rail-life.

Analysis of wheel-rail contact stresses shows that increasing of the wheel radius results increasing of the sinusoidal wheel-set path, the longitudinal elliptical semi-axis (A), decreasing of the contact stresses, and increasing of the rail life. Increasing of radius of curvature of the rails reduces the elliptical semi-axis (A), increases the contact stresses, and decreases the rail life. When the wheel

radius equals to the radius of curvature of the rail the contact area becomes a circle. Decreasing of the wheel load results reduction of the contact area, the contact stresses, and increasing of the rail life.

The investigation of the effects of the positions of the wheel contact on the contact area and contact stresses indicated that the minimum contact area and the maximum contact stresses occurs in case of flange contact (curved track), while the maximum contact area and minimum contact stresses occurs in case of moderate wheel shift (straight track).

The investigation of the effects of the positions of the wheel contact on the rail life indicates that the outer rails used in curves, which usually have flange contacts, have minimal life than rails used in straight track, which usually have moderates wheel shifts. The rails in straight track may have more than 1.5 fold of the lifetime than the rail in curved track.

References

[1] Klingel, "Ueber den Lauf der Eisenbahnwagen auf Gerader Bahn", Organ-Forschritter Eisenbahnwesen, Vol. 38, pp. 113-123 (1883).

[2] T.G. Pearce, "Wheelset Guidance-Conicity, Wheel Wear and Safety", Journal of Rail and Rapid Transit, Part F, Vol. 210, pp. 1-9 (1996).

[3] H. Hertz, "Ueber die Beruehrung fester elastische Koerper", Angewandte Mathematik, pp. 156-171 (1892).

[4] S. Iwnicki, "The Dynamic Behavior of Railway Vehicles with Solid Rubber Tires", Thesis submitted to the Council for National Academic Awards, South Bank Polytechnic, London (1991).

[5] Matsumoto, and K. Qi, "Wheel-Rail Contact Mechanics at full Scale on the Test Stand", Wear, Vol. 191, pp. 101-106 (1996).

[6] S.P. Timoshenko, and J.N. Goodier, "Theory of Elasticity", McGraw Hill, N.Y, pp. 403-420 (1970).

[7] J.H. Beynon, J.E. Garnham, and K.J. Sawley, " Rolling Contact Fatigue of Three Pearlitic Rail Steels", Wear, Vol. 192, pp. 94-111 (1996).

Received December 6, 2001
Accepted February 19, 2002